Nuclear Instruments and Methods in Physics Research B 269 (2011) 277–283

Contents lists available at ScienceDirect

Nuclear Instruments and Methods in Physics Research B

journal homepage: www.elsevier.com/locate/nimb

Roman bronze artefacts from *Thamusida* (Morocco): Chemical and phase analyses

E. Gliozzo [a,*], W. Kockelmann [b], L. Bartoli [c,1], R.H. Tykot [d]

[a] Dipartimento di Scienze della Terra, Università di Siena, via Laterina 8, 53100 Siena, Italy
[b] Science and Technology Facilities Council, Rutherford Appleton Laboratory, Harwell Science and Innovation Campus, Didcot OX11 0QX, United Kingdom
[c] Istituto dei Sistemi Complessi, Consiglio nazionale delle Ricerche, Via Madonna del Piano 10, 50019 Sesto Fiorentino (FI), Italy
[d] Department of Anthropology, University of South Florida, Tampa, FL 33620, USA

ARTICLE INFO

Article history:
Received 6 July 2010
Received in revised form 29 October 2010

Keywords:
Roman bronze
Thamusida (Morocco)
TOF-ND
Portable XRF

ABSTRACT

Twenty-six objects (1st to the 3rd century AD) found at the archaeological site of *Thamusida* (Morocco), which is a military settlement between the 1st and the 3rd century AD, have been investigated by means of portable X-ray fluorescence and time of flight-neutron diffraction. The combination of element-sensitive X-ray fluorescence and structure-sensitive neutron diffraction yields, in a totally non-destructive way, the necessary information to discriminate the copper alloy from corrosion and alteration layers. Results allowed dividing the repertory into five groups: (a) unalloyed copper, (b) binary alloys made of Cu and Sn, frequently leaded; (c) unleaded binary alloys made of Cu and Zn; (d) ternary alloys made of Cu, Sn and Zn, both leaded and unleaded; (e) quaternary alloys made of Cu, Sn, Zn and As. The choice of alloy is heterogeneous, mainly depending on availability and costs of raw and/or scrap materials and on technological constraints. Interestingly, the reconstruction obtained for *Thamusida* could either anticipate the important change in the Roman use of copper alloys generally referred as 'zinc decline', or more likely, indicate that brass never conspicuously entered the local metal-working activities of this military site.

1. Introduction

The copper-based artefacts recovered in Roman archaeological sites of northern Morocco (old province of *Mauretania Tingitana*) have been the subject of several catalogues and specific publications [1–3]. Archaeometric studies have been performed on a set of more than 150 items from *Volubilis*, *Sala*, *Banasa*, *Thamusida*, *Lixus* and *Tamuda*; however, the compositions obtained by optical spectrography are semi-quantitative (with errors around 50 wt.%), while X-ray fluorescence has been used for the characterisation of the alteration patina only [4].

In the light of the current state-of-the-art of the research on *Mauretania Tingitana*, the recovery of a further 300 copper-based objects from the archaeological site of *Thamusida* (Rabat, Morocco; Fig. 1) is of outstanding importance as it allows a comprehensive study of these artefacts from a well-dated Roman military site (1st–3rd century AD). Archaeological excavations at *Thamusida* ended in 2007. Therefore, the archaeological artefacts have not been published so far, with the exception of a military *diploma* [5,6]. The catalogue is in preparation, while the results of archaeometric investigations on a first sample set, including military and daily objects, are published in [7]. This second set of copper alloy materials was chosen in order to widen our knowledge on such artefacts from *Thamusida*, and to bring results into context in a wider perspective on history of productions and technologies.

The present study was motivated by the state-of-the-art investigations on Roman copper based artefact, and the stimulating perspectives offered by the combination of complementary non-destructive techniques: portable X-ray fluorescence spectrometry (PXRF) and time of flight-neutron diffraction (TOF-ND). PXRF is designed to perform spot chemical analyses directly on the object surface [8,9], therefore, it is particularly suitable to investigate the alteration patina and top corrosion layers on an object. In this sense, this technique provides a similar chemical analysis like particle induced X-ray emission (PIXE), although with a lower sensitivity for trace elements but with the advantages of being portable and providing immediate on-the-spot-analyses.

This technique provides an entirely non-destructive analysis. TOF-ND is a recognized non-invasive tool in archaeometallurgy for bulk quantitative phase and structure analyses of metals, for distinguishing preserved alloy phases from corrosion and alteration phases, and for providing micro-structural clues to discriminate between different working processes the object had been subjected

* Corresponding author.
E-mail addresses: gliozzo@unisi.it (E. Gliozzo), winfried.kockelmann@stfc.ac.uk (W. Kockelmann), bartoli@ifac.cnr.it (L. Bartoli), rtykot@usf.edu (R.H. Tykot).
[1] Present address: Istituto di Fisica Applicata "N. Carrara", Consiglio nazionale delle Ricerche, Via Madonna del Piano 10, 50019 Sesto Fiorentino (FI), Italy.

0168-583X/$ - see front matter © 2010 Elsevier B.V. All rights reserved.
doi:10.1016/j.nimb.2010.11.021

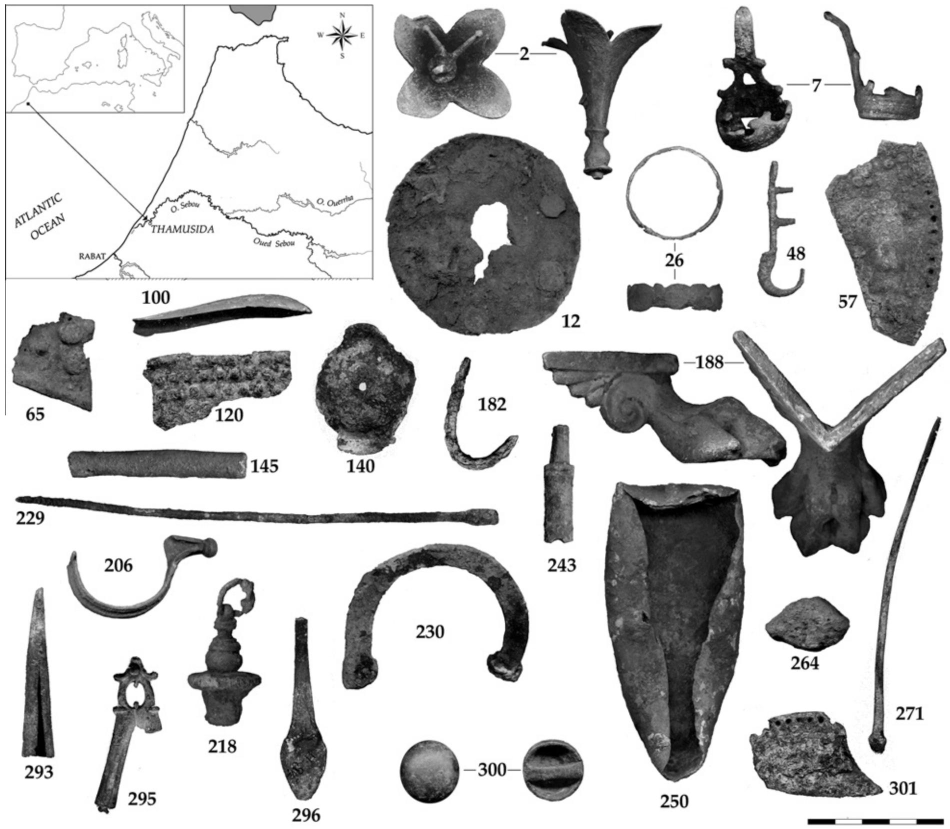

Fig. 1. Geographical position of the archaeological site of *Thamusida* (Rabat, Morocco) and photos of the investigated objects.

during manufacturing and use [10]. TOF-ND is able to overcome sampling problems encountered by conventional metallography, due to its deep penetration into the bulk of materials and the absence of invasive effects. Neutron beam sizes are big enough to illuminate large parts of an object, thus overcoming a major disadvantage of many conventional methods, where point sampling does not necessarily provide the characteristic material properties of the whole object. Providing phase-separated signals from the inner (unaltered alloy) as well as of the alteration layers, TOF-ND data are to a large extent insensitive to geometry and shape of the objects under examination, hence no preparation is needed. These latter advantages distinguish this technique to the conventional XRD instrument.

The study presented here is aimed at characterising object compositions by means of a scarcely-used combination of two non-destructive analytical techniques. The efficiency of this methodology has been validated by our previous study [7]. The characterisation of the object group from *Thamusida* will further provide key information on the bronze and brass production technology, and determine the conservation state of the collection. Technological information will be further exploited to relate composition vs. functional destination of each object here considered.

2. Materials

A set of 26 objects were selected for analysis on the basis of assumed object destination, function and type. The assemblage includes objects which can be surely related to the Roman army, or to daily objects that can be either associated to local inhabitants or military equipment (Table 1; Fig. 1). Military fittings include various types of harness fittings, a fragment of a parade helmet and an arrowhead. Sample THAM 264, which has been classified as a weight, could have been also used as a projectile. Daily objects are represented by (a) household goods, including furniture and vessel decorations and lamps, (b) ritual objects, which may also include THAM 296, (c) surgery and/or toilet tools, including a probe (*specillum* or stylet), a hair pin, objects used for body cleansing (*strigilis* or strigil) or for mixing soft substances (*spatula* or flat spoon), (d) clothing and jewellery, including a stud, a finger ring and objects for fixing leather and textile clothes, such as a brooch (*fibula*), and (e) few objects which can be ascribed to none or more than one of the above object classes, such as a bridle-bit, a fishing hook and a cymbal. In the process of cataloguing, the functions, typologies and chronologies of these objects will surely be more precisely specified. Therefore, some of the distinctions and classifications here adopted are open to revision.

The conservation states of the chosen objects for analysis has not primarily influenced its selection, but identifying and quantifying the corrosion state is rather a further objective of this study. Visually, the conservation state of the objects is variable, ranging from very altered (e.g. THAM 12, 140) to slightly altered (e.g. THAM 188, 300).

The collection, maintained by the Department of Archaeology and History of Arts of the Siena University, can be dated back to within the 1st–3rd centuries AD, corresponding to the permanence of the Roman army in the *Thamusida* settlement.

3. Experimental

3.1. Portable X-ray fluorescence

A Bruker Tracer III–V portable X-ray fluorescence spectrometer was used to analyze the metal artefacts. The flattest side of each artefact was subjected to an X-ray beam of 7 mm^2. Given the ab-

Table 1
Sample list. Weight expressed in grams.

Category	Inventory no.	Description	Weight
Group 1		Military	
	THAM 48	Loop	22
	THAM 65	Sheet (embossed decoration) (Parade helmet?)	12
	THAM 243	Strap end (*balteus*?)	18
	THAM 264	Weight/projectile	38
	THAM 293	Rounded socket/arrowhead	20
Group 2		Household goods	
	THAM 2	Flower	2
	THAM 12	Flat disk with raised centre	13
	THAM 57	Brim (vessel?)	17
	THAM 120	Sheet (embossed decoration)	11
	THAM 188	Lion shaped brazier/table foot	1
	THAM 218	Plug (*lucerna*?)	3
	THAM 230	Handle?	25
	THAM 250	Lamp (*lucerna*)	4
	THAM 295	Hold/handle	5
	THAM 301	Brim (vessel?)	39
Rituals	THAM 7	Ladle (*simpulum*)	6
Surgery and toilet	THAM 100	Strigil (*strigilis*)	10
	THAM 229	*Spatula*	14
	THAM 271	Pin	15
Jewellery and clothing	THAM 26	Finger ring	22
	THAM 206	Brooch (*fibula*)	9
	THAM 300	Stud	31
Varia	THAM 140	Cymbal	19
	THAM 145	Bridle-bit	37
	THAM 182	Fishing hook	36
	THAM 296	Spoon	16

sence of a perfect plane surface of an object, the penetration depth is in the range of 10–30 μm, also considering the lower penetration depth for several elements (e.g. iron). The instrument uses a thin Rh target in the X-ray tube, a Peltier cooled Ag-free SiPIN detector, and a Ti–Al filter to minimize certain peak overlaps. The settings selected for the present analyses were 40 kV and 4 μA with counting times of 30 s for each analysed point. Instrument calibration was achieved using a series of certified alloys (BCR 691, see [11]), available as a set of five polished discs of 35 mm diameter and 2 mm thickness, supplemented with a range of mixed alloy powder standards. Given that results provided by a spot analysis cannot be referred to the whole object and that the limited penetration implies that in some cases the alteration patina gives an overwhelming contribution to the analysis XRF signal, XRF data were only qualitatively interpreted. The data of 26 objects were used as guidance and for cross-checking the alloy compositions as obtained from the TOF-ND data.

3.2. Time-of-flight neutron diffraction

Bulk measurements of the objects were performed by TOF-neutron diffraction at the INES (Italian Neutron Experimental Station) and ROTAX beam-lines of the ISIS neutron source (Rutherford Appleton Laboratory, UK). ISIS is a pulsed source operating at 50 Hz (160 μA proton current). Neutrons are produced by stopping 800 MeV protons in a tungsten target clad with tantalum. The analysis of samples on both instruments is performed on stationary samples. Both instruments are able to accommodate relatively large objects which can be analysed in vacuum or air. Both instruments have detectors installed in the horizontal scattering plane at forward and backscattering angles. The energy-dispersive white-beam TOF technique facilitates the analysis of objects of complex shapes since each detector element provides a diffraction pattern with a series of Bragg peaks as a function of time-of-flight (TOF). The flight time (TOF) is related via Bragg's law and the de Broglie relationship to the crystallographic d-spacing (d):

$$\mathrm{TOF} = (m_n/h) * 2 * L * d * \sin\theta = 505.56 * L * d * \sin\theta \quad (1)$$

where TOF is measured in μs, L is the flight path from source to detector in meters, and the d-spacing is measured in Å. h is Planck's constant, m_n the mass of neutron, θ is the half-angle between the incident and diffracted beam directions, i.e. 2θ is the scattering angle. The peak width of Bragg peaks as a function of d-spacings is determined by the properties of the neutron moderator, by the sample thickness, and by microstructural properties of the sample. A special characteristic of TOF diffractometers is that the diffraction patterns recorded at backscattering angles is practically independent of the sample thickness. As a consequence, sharp diffraction lines can be obtained from thick objects in backscattering.

INES is installed on an ambient water moderator (316 K) with a maximum of the flux distribution around a neutron wavelength of about 1 Å. The neutron wavelength bandwidth ranges from 0.2 to 3.2 Å. The flight path from source to sample is 22.8 m. One hundred and forty four squashed 3He gas detectors are installed in a half-circle around the sample position in a distance of 1 m at scattering angles from 12° to 171°. INES is characterized by a diffraction resolution of 0.1% in backscattering and can access d-spacings up to 12 Å.

ROTAX views a cold liquid CH_4 moderator (110 K) with a maximum of the flux distribution around a neutron wavelength of about 2 Å. ROTAX uses neutrons between 0.5 and 5 Å at a flight path of 14 m from moderator to sample position. ROTAX uses two position-sensitive Li-glass scintillation detector banks covering 2θ ranges from 25° to 75° and 95° to 145°, respectively. ROTAX has a diffraction resolution of 0.4% in backscattering, and can access d-spacings up to 10 Å. For the measurements the objects were fixed with Al-tape on an aluminium frame and mounted in the sample chamber in the path of the neutron beam. For hollow objects a cadmium sheet was mounted inside the cavity to prevent scattering from the material on the backside, thus preventing double-diffraction patterns. An object was irradiated with a neutron beam of $4 \times 4\ \mathrm{cm}^2$ size (covering the whole object) on INES, and with a beam of $1.5 \times 3\ \mathrm{cm}^2$ cross section on ROTAX. Counting times were 3 h on both INES and ROTAX. After the measurements, the objects were stored in a lead case for a variable decay time never exceeding 48 h after which the activation had vanished below detectable limits.

Quantitative Rietveld analysis of the diffraction patterns (d-spacing range between 0.4 and 8 Å) was performed using the GSAS software [12,13] in order to refine lattice parameters of the copper alloys (Cu/Sn and Cu/Zn ratio; see [14,15]) and determine phase compositions. For the copper alloy phase the neutron scattering length of copper (7.7 fm) was used taking advantage of the fact that scattering lengths of Sn (6.2 fm) and Zn (5.6 fm) are relatively close to give sufficiently accurate copper alloy phase fractions. Reference structural models of cuprite, nantokite, malachite, quartz and calcite (symmetry, space group, lattice parameters, atom positions) were taken from the ICSD database (Inorganic Crystal Structure Database, Germany & National Institute of Standards and Technology, USA, 2004 [16]) and not further refined. The structure model of Pb, in particular the lattice parameter and the Debye Waller parameter, were obtained from the analysis of a pure Pb sheet.

One sample (THAM 12) was measured on both INES and ROTAX, i.e. on beamlines with different count rate and resolution characteristics, and with different beam sizes. The results give an indication of the systematic errors of lattice parameters and weight fractions of the TOF-ND analysis.

4. Results

PXRF data helped distinguishing between binary, ternary and quaternary alloys. Samples can be grouped as follows:

(a) unalloyed copper: THAM 229;
(b) binary alloy Cu–Sn (henceforth called unleaded bronze): THAM 26;
(c) binary alloy Cu–Sn + Pb (henceforth called leaded bronze): THAM 2, 7, 188, 243, 264;
(d) binary alloy Cu–Zn (henceforth called unleaded brass): THAM 65, 100, 206;
(e) ternary alloy Cu–Sn–Zn (henceforth called unleaded gunmetal): THAM 48, 120, 230, 250, 271, 293, 296, 301;
(f) ternary alloy Cu–Sn–Zn + Pb (henceforth called leaded gunmetal): THAM 12, 57, 145, 182, 218, 295, 300;
(g) quaternary alloy Cu–Sn–Zn–As (henceforth called quaternary alloy): THAM 140.

In this regard, it is worth emphasising that As is clearly present in THAM 140 only, but weak peaks have also been detected in THAM 12 and 182. Weak peaks of Fe are further present in all objects, but consistently present in samples THAM 206, 229, 264 and in the pistil of THAM 2.

Phase analysis was performed on all samples by TOF-ND (Table 2; Fig. 2) allowing both a measurement of the average lead contents, and the characterization of alteration phases and superficial incrustations.

Lead is absent in 11 samples (THAM 26, 48, 100, 120, 140, 229, 230, 250, 293, 296, 301), $\leqslant$1 wt.% in five samples (THAM 12, 65, 206, 271, 300), between 3.0 and 4.5 wt.% in four samples (THAM 57, 182, 218, 295), between 6 and 10 wt.% in two samples (THAM 145, 264), between 16 and 28 wt.% in four samples (2, 7, 188, 243).

Alteration phases are those generally detected at the surface layers of ancient bronzes, consisting of Cu salts generated in soil, in the atmosphere or in seawater (e.g. nantokite, malachite and atacamite). Nantokite and malachite are present in most unleaded alloys. Atacamite has been detected in four samples only, consisting of unleaded and low-lead gunmetal. It is generally accepted, at least for Cu–Sn alloys (see [17]), that phases above mentioned cover a cuprite layer that is in contact with the metal core. In fact, cuprite is always present, showing values particularly low for high-lead tin bronzes. The sums of alteration phases vs. Pb contents show that highly leaded tin bronzes are less altered than the other alloy types. Quartz and calcite have been randomly detected.

The two measurements performed on THAM 12 are a good example for the systematic error of the TOF-ND analyses made with different beamsizes (Table 2).

The Sn and Zn fractions were further determined from the TOF-ND data for bronzes and brasses from calibration curves using the refined lattice parameter of the copper alloy [14]. For gunmetals, i.e. copper alloys with more than one alloying element, the estimation of the element composition via Vegard's rule is ambiguous. However, it is still possible to determine an upper concentration limit for the presence of a given element.

Results provided in Table 3 show that the Sn wt.% content allows THAM 26 to be included in the group of unalloyed copper materials. Similar consideration may be applied for samples THAM 12 and 57, described as gunmetal by PXRF, with refined lattice parameters close to pure copper. Table 3 shows estimates for Sn and Zn contents for gunmetals THAM 12 and 57 on the assumption of binary Cu–Sn and Cu–Zn phases, in order to emphasize the low proportions of Sn and Zn in these alloys.

In high-lead bronzes (THAM 243, 2, 188 and 7) the copper alloy shows Sn values ranging from 7.6 to 10.4 wt.%. In brasses, the copper alloy exhibits Zn contents ranging from a minimum of 19.7 to a maximum of 21.7 wt.%. The diffraction patterns of THAM 100 indicate a large variation of the alloy composition by displaying broad structured alloy peaks. In this case, a Rietveld fit was carried out by including two copper alloy phases in the refinement model, representing minimum and maximum limits of a range of compositions.

Table 2
Results of multiphase analysis of 26 samples by TOF-ND. The lattice parameter of the copper alloy was refined in the Rietveld analysis. The statistical error bars of a lattice parameter are typically 0.0001 Å. The absolute weight ratios in the probed volume are reported. The error bars are of the order of 0.5 wt.%.

THAM #	Description	PXRF	Copper alloy		Lead	Cuprite	Nantokite	Malachite	Atacamite	Quartz	Calcite
			a (Å)	wt.%	wt.%	wt.%	wt.%	wt.%	wt.%	wt.%	wt.%
229	*Spatula*	Copper	3.6102	91.9	–	6.2	1.9	–	–	–	–
26	Finger ring	Bronze	3.6144	78.5	–	19.5	1.2	0.5	–	0.3	–
264	Weight/projectile	Bronze	3.6464	54.7	6.2	32.3	–	–	–	4.5	2.2
243	Strap end	Bronze	3.6589	71.0	28.1	0.9	–	–	–	–	–
2	Flower	Bronze	3.6701	83.3	16.2	0.5	–	–	–	–	–
188	Lion shaped foot	Bronze	3.6583	75.6	23.9	0.4	–	–	–	–	–
7	Ladle	Bronze	3.6747	70.4	25.5	4.1	–	–	–	–	–
206	Brooch	Brass	3.6595	86.1	0.1	13.8	–	–	–	–	–
65	Sheet	Brass	3.6621	92.0	0.2	7.8	–	–	–	–	–
100	Strigil	Brass	3.6641–3.6189	89.8–16	–	24.1	–	–	–	–	–
12	Flat disk	Gunmetal	3.6146	39.3	1.3	17.2	12.2	13.6	–	9.4	7
12	Flat disk	Gunmetal	3.6178	35.2	0.3	22.9	9.4	14.2	–	7.3	10.7
271	Pin	Gunmetal	3.6153	96.7	0.2	2.4	0.7	–	–	–	–
57	Brim	Gunmetal	3.6180	15.0	3.0	53.6	10.7	6.3	9.8	1.5	–
250	Lamp	Gunmetal	3.6199	74.7	–	14.1	8.4	–	2.7	–	–
230	Handle?	Gunmetal	3.6230	95.8	–	1.5	2.2	–	–	0.3	–
300	Stud	Gunmetal	3.6383	96.7	0.8	2.5	–	–	–	–	–
145	Bridle-bit	Gunmetal	3.6507	88.9	10.3	0.4	–	–	–	–	0.4
48	Loop	Gunmetal	3.6559	88.6	–	10.4	–	0.1	0.9	–	–
182	Fishing hook	Gunmetal	3.6622	38.6	3.1	58.2	–	–	–	–	–
296	Spoon	Gunmetal	3.6637	96.6	–	3.3	–	–	–	–	–
293	Arrowhead	Gunmetal	3.6677	79.2	–	20.8	–	–	–	–	–
218	Plug	Gunmetal	3.6727	90.2	3.1	4.2	2.5	–	–	–	–
295	Hold/handle	Gunmetal	3.6756	92.9	4.5	2.5	–	–	–	–	–
120	Sheet	Gunmetal	3.6729	81.9	–	18.1	–	–	–	–	–
301	Brim	Gunmetal	3.6989	17.3	–	52.6	6.6	11.4	10.6	1.5	–
140	Cymbal	Cu–Sn–Zn–As	3.6449	78.6	–	16.6	4.6	–	–	–	–

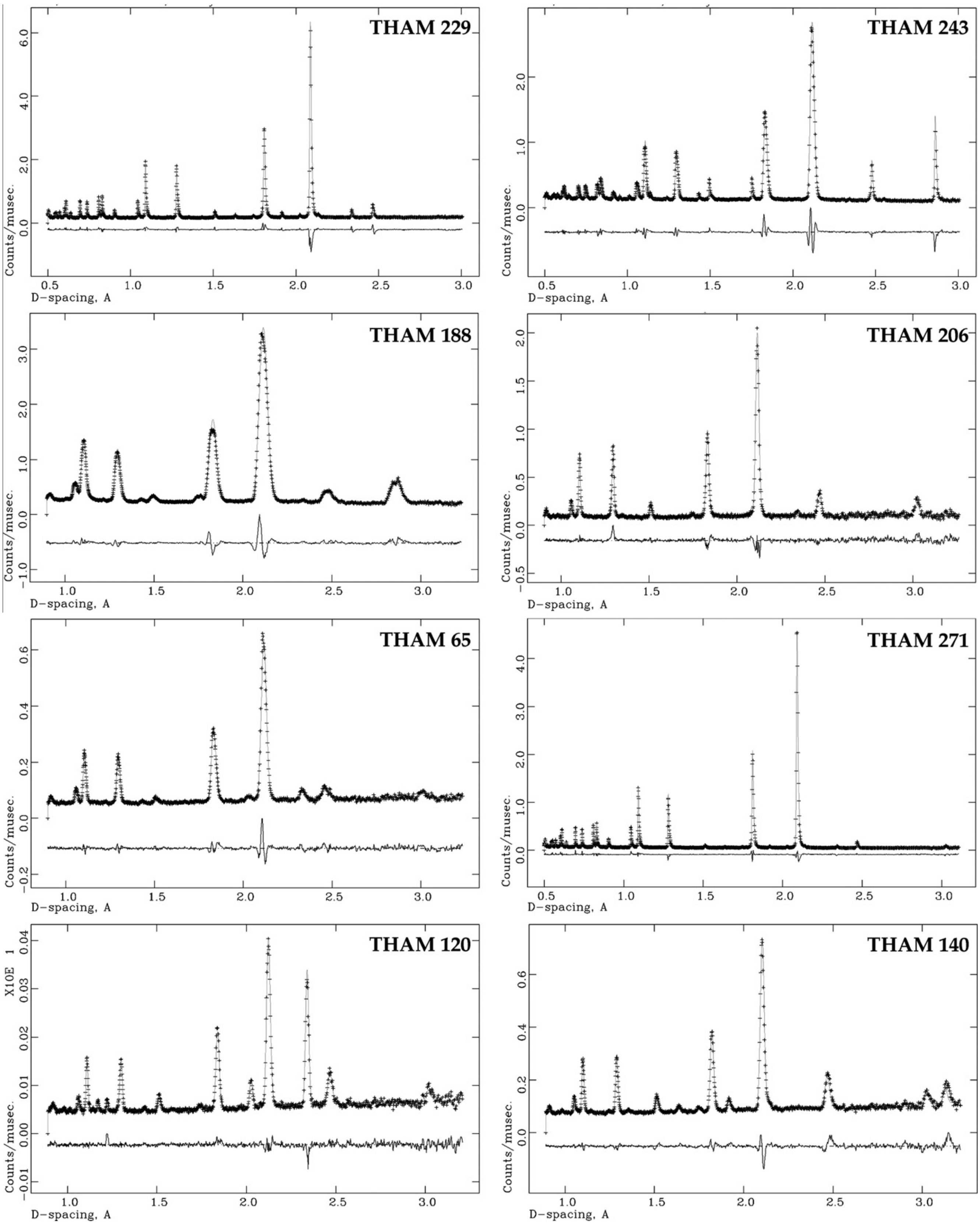

Fig. 2. Rietveld refinements of diffraction patterns from unalloyed copper (THAM 229), bronzes (THAM 243 and 188), brasses (THAM 206 and 65), gunmetals (THAM 271 and 120) and the quaternary alloy (THAM 140).

Table 3
Estimated Sn and Zn contents, derived from calibration curves using the refined lattice parameters of the copper alloys. For THAM 12 and THAM 57, identified as gunmetals by PXRF, upper limits for both Sn and Zn concentrations are calculated from the refined TOF-ND lattice parameters and given in parentheses.

THAM #	Description	PXRF	Copper alloy	Bronze		Brass	
			a (Å) refined	Cu (wt.%)	Sn (wt.%)	Cu (wt.%)	Zn (wt.%)
26	Finger ring	Copper	3.6144	99.8	0.2		
264	Weight	Bronze	3.6464	94.4	5.6		
243	Strap end	Bronze	3.6589	92.3	7.8		
2	Flower	Bronze	3.6701	90.4	9.6		
188	Lion shaped foot	Bronze	3.6583	92.4	7.6		
7	Ladle	Bronze	3.6747	89.6	10.4		
206	Brooch	Brass	3.6595			80.3	19.7
65	Sheet	Brass	3.6621			79.1	20.9
100	Strigil	Brass	3.6189			98.0	2.0
			3.6641			78.3	21.7
12	Flat disk	Gunmetal	3.6146	(99.7)	(0.3)	(99.2)	(0.8)
12	Flat disk	Gunmetal	3.6178	(99.2)	(0.8)	(97.8)	(2.2)
57	Brim	Gunmetal	3.6180	(99.1)	(0.9)	(97.7)	(2.3)

5. Discussion

Based on metal compositions of the analysed objects, our study described a heterogeneous context. Unalloyed copper, i.e. a rather soft and malleable metal of pinkish red colour, was used for few items such as the *spatula* (THAM 229) and the finger ring (THAM 26). It is worth noting the low quality of the latter item, based on the fact that, in Roman times, plain rings were usually made of gunmetal, with high Pb content [18].

In the flat disk THAM 12, the brim THAM 57 and the lamp THAM 250, there are no significant quantities of alloying elements detected in the copper alloy. These objects could be either classified as unalloyed copper or involuntary copper alloys. Dungworth [18] noticed that bronzes with tin contents of around 1–5 wt.% were widely used for sheet and wire objects, being mechanically very similar to pure copper; this observation is in good agreement with our results. However, results obtained for the lamp are rather unusual. In their study of copper-alloy lamps from about 600 BC to 800 AD, Hook and Craddock [19] found only for four lamps out of 550 analyses Cu contents above 95 wt.% (nos. 3537, 3782, 3839, 3840) and only one with Cu content above 98 wt.% (no. 3838: Cu 98.3 wt.%, Pb 1.20 wt.%), while most of the analysed collection was made of bronze or, to a lesser extent, of brass, both frequently leaded.

A small group of objects is made of leaded bronze: the weight (THAM 264), the strap end (THAM 243), the flower (THAM 2), the lion shaped foot (THAM 188) and the ladle (THAM 7).

Tin percentages in the alloys are above 5 wt.%, hence it is likely that its introduction was intentional [20]. It is well known that the addition of tin to copper has numerous advantages: increase of the hardness of the metal, lowering of the temperature of the melt (e.g. 1085 °C for pure copper against ~1000 °C for a copper alloy with 10 wt.% Sn), easier casting procedure by increasing the fluidity of the molten metal, conferment of a golden appearance to the object (see, e.g. [21,22]). The correlation between alloy type and object destination and function works rather well. The weight did not require a particular hardness or a golden appearance; in fact, it shows the lowest values of tin. Conversely, easy casting, hardness and golden appearance could have been sought for the production of the lion shaped foot and the strap end, showing intermediate tin values (7.6 wt.%), and the flower and the ladle, showing the highest tin values (9.6 and 10.4 wt.%, respectively).

The other advantages of tin addition, i.e. lower working temperature and easier casting, are somehow shared with lead; for instance, the melting temperature of a bronze can drop to less than 800 °C with the addition of about 25 wt.% Pb [23]. In all bronzes, lead was intentionally added, showing variable contents between 10 and 29 wt.% [22]. The technical advantages of decreasing the viscosity of the molten metal during casting without detracting the strength of the alloy, should have been particularly aimed for the production of complex cast objects [24], such as the flower, the lion shaped foot and the ladle. It is important to remind that lead helps casting but complicates hammering, as it does not enter the alloys, segregating separately in droplets (see, e.g. [18,22]); hence, the high contents of lead in the strap end are not easily justifiable. Lastly, lead was cheaper and denser than tin, hence it had the property of increasing the weight of the object, decreasing production costs (see, e.g. [19]). In this regard, however, it is worth noting that the weight THAM 264 is the one with the lowest content of lead among these bronze objects.

Another even smaller group of materials is made of unleaded brass: the sheet decoration THAM 65, the strigil THAM 100, and the brooch THAM 206.

Suitable for casting and hammering, indeed brass was technically appropriate for the production of these objects. The variable contents of Zn are important in order to hypothesise whether cementation brasses (with 15–28 wt.% Zn; see [25,26]) or remelted brass (decreasing Zn content due to volatilisation) has been used [19,25,27–30]. Showing high Zn contents, the three investigated brass objects should be then described as cementation brasses. In this regard it is worth reminding that the thesis stating brass production as a state monopoly [27,31,32] found a robust argument in the fact that Roman military brasses were predominantly cementation brass, with Zn average contents higher than those of civilian brooches [19,26,29]. However, the analyses of 1212 Roman copper alloys by Dungworth [18] show that the availability of brass is not always related to Romanised sites, being abundant in the indigenous manufacture of small rural sites. The scenario depicted by the analyses of *Thamusida* artefacts is rather different from those generally shown for military sites, since only a very small percentage of items is made of brass: 12% in the present research, none in the previous study on 22 copper alloys from *Thamusida* as well [7]. With Cowell et al. [33], it is maybe possible to list *Thamusida* within the areas where brass was slowly adopted and bronze was continuously used over centuries. Still, the high Zn content in *Thamusida* brasses is remarkable, as such high values are scarcely represented in Roman alloys [18]. Lastly, it is possible to hypothesise that high peaks of iron (detected with XRF) in THAM 206 could suggest the use of smithsonite in making brass. In fact, iron contents below 0.25 wt.% are generally referred to as impurity while higher levels should suggest the use of smithsonite [21,34,35]. Unfortunately, this hypothesis cannot be verified since manganese, which has been identified as a diagnostic feature of smithsonite brass (see also [36]), has not been detected by PXRF in our samples.

Most of the analysed samples are made of leaded and unleaded gunmetal: the loop THAM 48, the sheet decoration THAM 120, the bridle-bit THAM 145, the fishing hook THAM 182, the plug THAM 218, the arrowhead THAM 293, the handle THAM 295, the spoon THAM 296, the stud THAM 300 and the brim THAM 301. Considering both function and destination of these objects it is clear that the choice of the alloy type is unrelated to a specific technical issue, except maybe for lead. For instance, spoons, sheet decorations or flat brims were frequently wrought instead of cast, requiring thus low Pb contents.

The survey of the Roman copper alloys provided by Dungworth [18] shows that from the 1st century AD, this ternary alloy (leaded or unleaded) was increasingly used, together with leaded bronze, provoking a decreasing amount of brass and leaded brass objects. The author further adds that brass was rarely recycled on its own but mixed with bronze (instead of Sn) and that lead was mainly introduced by bronze itself instead of being separately added. In the analysed objects, recycling must have been frequent, given that lead contents are below the limit of the intentional addition in most cases (see [22]).

Lastly, sample THAM 140 shows a quaternary alloy made of copper, tin, zinc and arsenic. The presence of arsenic is not surprising as about 15% of Roman alloys contain this component [18]. The lack of absolute values for each component does not allow further considerations on this topic, however, it is maybe important to underline that, similarly to tin, arsenic permits better casting than pure copper and analogously to gunmetal, the introduction of arsenic in quaternary alloys should be correlated to the remelting of copper alloys instead of the addition of refined arsenic.

6. Conclusions

The studied collection is quantitatively numerous and typologically heterogeneous, including military fittings, household goods, ritual and surgery instruments, toilet and clothing articles, jewellery and numerous objects which can be ascribed to a specific function (e.g. *lucernae*, studs, cymbals, fishing hooks, etc.) but not to a social group (i.e. civilian or army).

The choice of the alloy is heterogeneous as well, depending on availability and costs of raw or scrap materials and on technological constraints.

It is interesting to note that available reconstructions on the chronological changes in copper alloys demonstrated that the 'decline' of brass in favour of leaded bronze and gunmetal should be dated back to around the 4th century AD. The overall situation reconstructed for *Thamusida*, which is a military settlement between the 1st and the 3rd century AD, seems to fairly anticipate this important change in the production and use of copper alloys. The majority of samples are gunmetals (48%), followed by a smaller quantity of bronze (20%) and few examples of brasses (12%). It is important to note that unalloyed copper is rather abundant (20%) if compared to other military sites. Another feasible explanation is that brass never conspicuously entered the local metal-working activities of this military site.

Despite the fact that this final scenario could be compromised by the effective representativeness of our collection, we would like to note that relatively few collections of copper-based objects have been systematically characterized so far. The final reconstruction is far from being established, especially when considering that entire provinces like the *Mauretania Tingitana* have never been studied before.

Lastly, material provenance was not under investigation but it is interesting to consider that the Roman province of *Mauretania Tingitana* was thought to entertain most of its trades with southern-Spain, the latter being one of the two principal areas of metal production in the Roman Empire (the second was the *Britannia*). However, the richness of ore sources in Morocco should be considered as well, even in the total absence of studies on this topic.

References

[1] C. Boube-Piccot, Bulletin d'Archéologie Marocaine 5 (1964) 145–181.
[2] C. Boube-Piccot, Bulletin d'Archéologie Marocaine 17 (1987–1988) 209–229.
[3] C. Boube-Piccot. Bronzes antiques: productions et importations au Maroc, in: P. Trousset (Ed.), L'Afrique du Nord antique et médiévale, VIe Colloque international sur l'histoire et l'archéologie de l'Afrique du Nord. Productions et exportations africaines. Actualités archéologiques (Pau, octobre 1993), Editions du CTHS, Paris, 1995, pp. 65–77.
[4] C. Boube-Piccot, Etudes et travaux d'Archeologie Marocaine 4 (1969) 382.
[5] E. Papi, Zeitschrift für Papirologie und Epigraphik 142 (2003) 257–266.
[6] E. Papi, Zeitschrift für Papyrologie und Epigraphik 146 (2004) 255.
[7] E. Gliozzo, R. Arletti, L. Cartechini, S. Imberti, W.A. Kockelmann, I. Memmi, R. Rinaldi, R.H. Tykot, Journal of Applied Radiation and Isotopes 68 (2010) 2246–2251.
[8] M. Milazzo, Nuclear Instruments and Methods in Physics Research Section B 213 (2004) 683–692.
[9] A.G. Karydas, D. Kotzamani, R. Bernard, J.N. Barrandon, Ch. Zarkadas, Nuclear Instruments and Methods in Physics Research Section B 26 (2004) 15–28.
[10] E. Pantos, W.A. Kockelmann, L.C. Chapon, L. Lutterotti, S.L. Bennet, M.J. Tobin, J.F.W. Mosselmans, T. Pradell, N. Salvado, S. Buti, R. Garner, A.J.N.W. Prag, Nuclear Instruments and Methods in Physics Research Section B 239 (2005) 16–26.
[11] C. Ingelbrecht, A. Adriaens, E. Maier, Certification of Arsenic, Lead, Zinc and Tin (Mass Fractions) in Five Copper Alloys, BCR 691, Report EUR 19778/1, 2001.
[12] A.C. Larson, R.B. Von Dreele, General Structure Analysis System (GSAS), Report LAUR 86-748, Los Alamos National Laboratory, 2000
[13] B.H. Toby, Journal of Applied Crystallography 34 (2001) 210–213.
[14] S. Siano, L. Bartoli, M. Zoppi, W.A. Kockelmann, M. Daymond, J. Dann, M. Garagnani, M. Miccio, Proceedings of Archaeometallurgy Europe 2 (2003) 319–330.
[15] S. Siano, L. Bartoli, W.A. Kockelmann, M. Zoppi, M. Miccio, Physica B 350 (2004) 123–126.
[16] <http://www.fiz-informationsdienste.de/en/DB/icsd/index.html>.
[17] I. Constantinides, A. Adriaens, F. Adams, Appl. Surf. Sci. 189 (2002) 90–101.
[18] D.B. Dungworth, 1997. <http://intarch.ac.uk/journal/issue2/dungworth_index.html>.
[19] D.R. Hook, P.T. Craddock, The scientific analysis of the copper-alloy lamps: aspects of classical alloying practices, in: D.M. Bailey (Ed.), A Catalogue of the Lamps in the British Museum. IV. Lamps of Metal and Stone and Lampstands, British Museum Press, London, 1996, pp. 144–164.
[20] H.H. Coghlan, Occasional Papers on Technology, Pitt Rivers Museum, Oxford, 1975 (Chapter 4).
[21] M. Ponting, I. Segal, Archaeometry 40 (1998) 109–122.
[22] H. Unglik, Archeomaterials 5 (1991) 91–110.
[23] J. Young, The Addition of Lead to Alloys in the Late Bronze Age, Unpublished B.Sc. Dissertation, University of Oxford, 1967.
[24] J.A. Smythe, Proceedings of the University of Durham Philosophical Society 9 (1936) 382–405.
[25] I. Jenkins, Britannia 16 (1985) 141–164.
[26] R.P.J. Jackson, P.T. Craddock, in: B. Raftery, V. Megaw, V. Rigby (Eds.), Sites and Sights of the Iron Age, Oxbow Monograph, vol. 56, Oxbow Books, Oxford, 1995, pp. 75–102.
[27] E.R. Caley, Orichalcum and Related Ancient Alloys. Origin, Composition and Manufacture with Special Reference to the Coinage of the Roman Empire, New York, 1964.
[28] P.T. Craddock, Journal of Archaeological Sciences 5 (1978) 1–16.
[29] J. Bayley, in: D.S. Neal, A. Wardle, J. Hunn (Eds.), Excavation of the Iron Age, Roman and Medieval Settlement at Gorhambury, English Heritage Archaeological Report, vol. 14, English Heritage, London, 1990.
[30] P.T. Craddock, Early Metal Mining and Production, Edinburgh University Press, Edinburgh, 1995.
[31] M. Grant, From Imperium to Auctoritas: A Historical Study of Aes Coinage in the Roman Empire, 49 BC–AD 14, Cambridge University Press, Cambridge, 1946.
[32] M.C. Bishop, J.C.N. Coulston, Roman Military Equipment from the Punic Wars to the Fall of Rome, Oxbow books, Oxford, London, 1993.
[33] M.R. Cowell, P.T. Craddock, A.W.G. Pike, A.M. Burnett, in: B. Kluge, B. Weisser (Eds.), Proceedings of the 12th International Numismatic Congress (Berlin 1977), Philip von Zabern, Berlin, 2000, pp. 670–677.
[34] P.T. Craddock, A. Burnett, K. Preston, W.A. Oddy, British Museum Occasional Paper 18 (1980) 53–64.
[35] P.T. Craddock, S.C. La Niece, D.R. Hook, British Museum Occasional Publication 50 (1998) 73–114.
[36] I. Carradice, M.R. Cowell, Numismatic Chronicle 147 (1987) 69–80.